Unilateral ephaptic program underlying sweetness dominance

MinHyuk Lee[1,3,4], Seon Yeong Kim[1,2], Taeim Park[1], Kyeung Min Joo[3], Jae Young Kwon[4], Kyuhyung Kim[2] and KyeongJin Kang[1*]

[1]Neurovascular unit research group, Korea Brain Research Institute, Daegu, 41062, Republic of Korea.

[2]Department of Brain Sciences, DGIST, Daegu, 42988, Republic of Korea.

[3]Department of Anatomy and Cell Biology, Sungkyunkwan University School of Medicine, Samsung Biomedical Research Institute, Samsung Medical Center, Suwon, 16419, Republic of Korea.

[4]Department of Biological Sciences, Sungkyunkwan University, Suwon, 16419, Republic of Korea.

*Corresponding author. Email: kangkj@kbri.re.kr

Abstract: Ephaptic coupling is a unique way physically adjacent neurons can influence one another's activity that, without an underlying molecular mechanism, could easily be considered a form of electrical interference rather than a genuine contributor to information processing. Here, we show the hyperpolarization-activated cyclic nucleotide-gated (HCN) channel unilateralizes the ephaptic inhibition of *Drosophila* gustatory receptor neurons (GRNs). HCN in sweet-sensing GRNs (sGRNs) allows sweetness to dominate bitterness. Simultaneously, HCN, throttling sGRNs in sugar-rich environments, enhances bitter-sensing GRN sensitivity to allow for uncompromised aversion to potentially toxic bitter substances. Thus, ephaptic inhibition can be genetically programmed and subjected to natural selection. This implies ephaptic coding arose to meet a physiologic need and may provide mechanistic insights into the well-known but enigmatic phenomenon of sweet-dependent taste suppression in humans.

Introduction

Electrical activity in the form of action potentials mediates intraneuronal signal propagation. This can lead to extracellular potential changes that increase or decrease the excitability of adjacent neurons independent of any synapses, a phenomenon called ephaptic coupling(1–3). Although the mechanisms underlying ephaptic coupling and their implications are unclear, the phenomenon is ubiquitous in the brain(4–7) and thought to underlie the temporal synchronization of neuronal firing that generates neural oscillations(4,5,8). Such coupling can be dramatic when two neurons form complex interfaces like the pinceau formed between basket cells and Purkinje neurons in mice (9), the axon cap formed between PHP interneurons and Mauthner cells in fish (10), and those formed among the compartmentalized olfactory receptor neurons (ORNs) in *Drosophila* (11–13). All these cases are examples of ephaptic inhibition(3). The latter two examples are characterized by bilateral inhibition between the participating neurons(12,14,15). Interestingly, differences in cell size lead to asymmetric lateral suppression, with larger *Drosophila* ORNs dominating their smaller partners (12). Ephaptic inhibition occurs when excitation of a neuron hyperpolarizes a partner target neuron (3,9,12). We still understand little about the genetic programming and regulation of ephaptic coupling beyond its most basic features, such as structural complexity and hyperpolarization of the inhibited neurons.

Carbohydrates, the primary energy source for animals, are produced by plants and other photosynthetic organisms. Sugar-producing organisms often deter predators with bitter compounds that warn animals of potential post-ingestive toxicity (16). To avoid the toxicity, sugar ingestion in *Drosophila* has been reported to be suppressed in the presence of bitters (17–21). This can be achieved by two distinct mechanisms, the odorant-binding protein OBP49a(21) and a GABA-mediated inhibitory circuit(17). At the same time, animals must overcome the bitter-induced aversion to feed on bitter-laced sugars. Human gustation is largely tuned to favor sugar ingestion, with sweetness reducing the perception of other primary taste modalities in psychophysiological studies (22–29). Yet, little is known about the sensory processing mechanisms underlying sweetness dominance. In *Drosophila*, their phytophagy suggests the existence of a system for sugar-induced bitterness suppression to facilitate adequate carbohydrate intake, but, as in other animals, the mechanisms of sweetness dominance in *Drosophila* remain unclear. Here, we describe how ephaptic inhibition between sweet- and bitter-sensing gustatory receptor neurons (s- and bGRNs) is unilateralized to encode firm sweet-dependent bitter taste suppression.

Results

Sucrose inhibits bitter sensing and avoidance.

Serendipitously, we observed that extracellular recordings of labellar bristle sensilla with bitter/sucrose mixtures produced significantly smaller responses from bGRNs than bitter-only controls (Fig. 1A,B, and fig. S1A,B). Both i- and s-type labellar bristle sensilla house a bGRN and an sGRN (Fig. 1A) (30–32). The spiking responses from the sensilla of WT (cantonized w^{1118}) in response to bitter/sweet mixtures were readily discernible into two categories based on spike amplitude in both the depolarization and repolarization phases (fig. S1A). To control for any effect of osmolarity, the bitter-only control solution contained equimolar sorbitol, which is nonsweet to flies (33). Sucrose suppressed responses to various bitters that stimulate both i- and s-type labellar bristle sensilla, indicating that sucrose-dependent inhibition is common to bGRNs regardless of bristle type (Fig. 1A-D, fig. S1B). We found that glycerol, which stimulates sGRNs (34), also suppressed bGRN activity (fig. S1C,D). Next, we examined the behavioral significance of this spiking suppression using capillary feeder (CAFE) assays (35,36) in which flies were offered two capillaries containing the same concentration of sucrose plus or minus a bitter

compound. We found increasing concentrations of sucrose reduced bitter avoidance (Fig. 1E-G), indicating that sweetness suppresses the feeding avoidance induced by bitter chemicals. This inhibitory effect was not due to increased osmolarity, however, because equi-osmolar substitutions of sucrose with nonsweet sorbitol restored the avoidance (Fig. 1F,G).

Sucrose-induced bitterness suppression requires sGRN excitation but not chemical synaptic transmission.

Next, we asked whether the lateral inhibition requires sucrose sensing by the sGRNs. The *Gr64af* deletion mutant lacks the entire *Gr64* gene locus from *Gr64a* to *Gr64f* and cannot detect sucrose(34). In the i- and s-type sensilla of *Gr64af* mutants, the bitter/sucrose mixture elicited spiking responses only from bGRNs. We found that the addition of sucrose to a bitter tastant elicited a similar bGRN response as the bitter-only control (Fig. 2A, fig. S2A). In CAFE assays, increasing concentrations of sucrose did not produce any significant suppression of bitter avoidance in *Gr64af* mutants (Fig. 2B). We next used *Gr5a-Gal4* (37) to drive the overexpression of the inwardly rectifying potassium channel Kir2.1 (38) to silence sGRNs with temporal control provided by *Gal80*^{ts} (Fig. 2C) (39). When we activated the silencing in adults by raising the temperature to 29°C, the sucrose-induced inhibition of caffeine-activated bGRNs was abolished (Fig. 2C, fig. S2B). In contrast, blocking chemical presynaptic transmission in sGRNs by similarly expressing the tetanus toxin light chain (TNT)(40) did not relieve sucrose-dependent bGRN inhibition (Fig. 2D, fig. S2C). We then confirmed these electrophysiological findings in CAFE assays, where blocking action potentials, but not chemical synaptic transmission, allowed the persistence of caffeine avoidance even in the presence of 350 mM sucrose (Fig. 2E). We next used RNAi in bGRNs to knock down the inhibitory neurotransmitter receptor genes *rdl* (41) and *gluClα* (42), which mediate fast GABAergic and glutamatergic postsynaptic inhibition, respectively. Additionally, in sGRNs, we targeted *shakB,* which encodes a major neuronal gap junction channel (43). None of these knock-down experiments resulted in significant electrophysiological impairment of the lateral inhibition between GRNs (fig. S3). These results suggest that peripheral sGRN excitation, and not synaptic feedback to bGRNs, is required for lateral bGRN inhibition.

Optogenetic excitation of sGRNs inhibits bGRNs.

Inhibition of sGRNs in L-type bristles requires the odorant-binding protein OBP49a, which is thought to bind various bitter compounds (21). To determine whether OBPs contribute to sweet-dependent bGRN inhibition, we used an optogenetic approach with red activatable channelrhodopsin (ReaChR) (44) in combination with extracellular recordings (Fig. 3A,B). After applying a series of ten 0.1-sec orange light pulses at intensities ranging from 1 to 50 mW/cm^2 10 sec after initial contact with N-methyl maleimide (NMM), we measured bGRN spiking frequencies for 0.9 sec after each light pulse. NMM is an irreversible activator of TRPA1, which is natively expressed in bGRNs. As such, NMM generated sustained spiking responses (36). Activation of sGRNs by light stimulations of as low as 5 mW/cm^2 significantly decreased the bGRN firing induced by 2 mM NMM, but maximal inhibition was achieved with stimulations of 25 mW/cm^2 (Fig. 3B). The duration of the bGRN inhibition showed a monotonic correlation with increasing illumination intensity and time (fig. S4B,C). In addition, we obtained similar results with caffeine and theophylline, which activate bGRNs in other bristle sensilla (Fig. 3C,D). From these results, we can conclude that the lateral inhibition of bGRNs we observed with optogenetic

excitation of sGRNs does not require OBPs, and that the inhibition can be both rapid and prolonged.

The inhibiting sGRNs are smaller than the bGRNs they inhibit.

Ruling out the involvement of synaptic transmission and OBPs, we began to consider ephaptic coupling as the mechanistic basis for this lateral inhibition, in part because ephaptic coupling has been reported in ORNs (11,12). Zhang et al. showed that spike amplitudes generally correlate with the relative cell size of the ORNs co-housed in a single sensillum, with the larger cells producing taller spikes. The larger ORNs readily suppress the smaller ORNs, resulting in an asymmetric ephaptic interaction (12). Intriguingly, our sensillar recordings of GRN activity seem to show the opposite relationship with the sGRN that is inhibiting the bGRN producing the shorter spikes (Fig. 1, fig. S1A). To determine whether the larger cells produce the shorter spikes in the case of GRNs, we performed volumetric/morphometric analyses on 3D confocal images taken from flies with adjacent s- and bGRNs marked with different membrane-tethered fluorescent proteins (i.e., mCD8-GFP or mCD8-RFP) (Fig. 3E). We collected data only from GRN pairs with a voxel intensity difference of less than 10% (Fig. 3F, middle). The bGRN cell body volumes (mean ± SEM: 0.177 ± 0.033 mm^3) averaged roughly two-fold larger than those of the sGRNs (0.086 ± 0.009 mm^3, Fig. 3F, left). In other words, sGRN soma volume was like that of the large ORNs(12,45). We did not see any correlation between the measured volume difference and the voxel intensities (Fig. 3F, right), excluding the possibility that our measurements were biased by differences in fluorescence intensity. Therefore, we conclude that, as with ORNs, spike heights are a reliable way of approximating the relative cell size of neighboring GRNs. This is presumably due, at least in part, to a similar distance of the recording electrode from the sites of origin for the action potentials in each neuron type. Thus, we confirmed that the smaller sGRNs exert lateral inhibition on the larger bGRNs.

Lateral inhibition between sGRNs and bGRNs is unilateral against the cell size gradient.

We next asked whether ephaptic inhibition between GRNs is bilateral, with the opposite direction (bGRN-dependent sGRN suppression) being more robust due to the size gradient, as it is in ORNs. To this end, we subjected sGRNs to lateral inhibition by optogenetically activating bGRNs. We did this while also ectopically expressing TRPA1 in the *TrpA1*-deficient mutant $TrpA1^{ins}$(46) to generate sustained sGRN spiking in response to NMM (Fig. 3G,H). Strikingly, we did not observe any inhibition of NMM-activated sGRNs induced by optogenetic excitation of bGRNs even at the highest level of irradiance (100 mW/cm^2). We also confirmed this result with sucrose-activated sGRNs (Fig. 4C,D), strongly suggesting that the ephaptic interactions between GRNs are unilateral against the cell size gradient.

Ih is required for unilateral inhibition, and lack of Ih results in bilateral interaction.

In searching for the mechanism underlying unilateral inhibition between GRNs, we hypothesized that the hyperpolarization imposed on sGRNs by bGRN activation could be negated by a hyperpolarization-induced mechanism that counteracts it. This would manifest in a lack of ephaptic inhibition of sGRNs by bGRNs, leaving only the inhibition of bGRNs by sGRNs. We reasoned that HCNs may provide such a mechanism because they depolarize the membrane by conducting Na^+ and K^+ upon hyperpolarization. This would potentially relieve sGRNs from any hyperpolarizing inhibition. Although the human HCN family comprises four members (47), the *Drosophila* genome encodes only one HCN orthologue from the *Ih* locus that shares biophysical properties with mammalian HCNs in heterologous expression systems (48). Ih^{f03355} is a strong loss-of-function allele in which the *Ih* gene is disrupted by a transposon

insertion (49,50). Interestingly, in *Ih*^{f03355}, unlike WT, sucrose did not reduce bGRN responses to caffeine (Fig. 4A,B, fig. S5A). Furthermore, the direction of lateral inhibition between the GRNs appeared to be reversed, with *Ih*^{f03355} showing reduced sucrose-induced sGRN spiking in the presence of caffeine. Introduction of a genomic fragment containing the *Ih* locus ({*Ih*}) rescued these impairments, confirming that HCN is required for sweet-dependent bGRN inhibition. Corroborating this result, we found that, in contrast to WT, optogenetic excitation of *Ih*^{f03355} bGRNs expressing ReaChR under the control of *Gr66a-LexA* (51) inhibited sucrose-stimulated sGRNs (Fig. 4C,D) regardless of bristle type (fig. S5B). We next attempted to suppress HCN activity using the well-known chemical inhibitor zatebradine (ZB) (52). Bristle sensilla of interest were pre-exposed to either water (mock) or 10 mM ZB for 2 min, immediately followed by optogenetic extracellular recording. In flies exposed to ZB, optogenetic activation of bGRNs suppressed sucrose- and NMM-induced sGRN spiking, the latter of which was accomplished via TRPA1 expressed in *TrpA1*-deficient sGRNs under the control of *Gr5a-Gal4* (*32*) (Fig. 4E,F). This pharmacological result suggests the defect we observed in *Ih*^{f03355} was neither developmental nor remotely inflicted. The relative GRN spike heights in *Ih*^{f03355} flies were like those of WT, suggesting that the size gradient between the GRNs persisted in *Ih*^{f03355} (Fig. 4A). Next, we asked whether the bGRN suppression induced by optogenetic sGRN activation was abolished in *Ih*^{f03355} (Figure 4B). Interestingly, sGRN excitation via ReaChR readily reduced caffeine-induced bGRN responses in *Ih*^{f03355} (Fig. 4G,H, fig. S5C), indicating that ephaptic coupling between GRNs is bilateral in the absence of functional *Ih*. The apparent reversal of the unilateral inhibition with chemically excited GRNs in Fig. 4A,B suggests that the balance of the GRN interaction in the mutants shifted toward dominance by the large bGRNs. The resulting situation is like the asymmetrical, bilateral size-dependent inhibition reported for ORNs (12).

Ih expression in sGRNs is required for unilateral inhibition.

Our hypothesis is based on the putative expression of HCN in sGRNs. Next, we performed optogenetic extracellular recordings using flies with GRN-specific RNAi knockdown of *Ih*. Driving *Ih* RNAi in sGRNs using *Gr64f-Gal4*(54) allowed similar bilateral inhibition (Fig. 5A) to what we observed with *Ih*^{f03355} flies (Fig. 4), indicating that *Ih* is required in sGRNs for unilateral inhibition. Driving *Ih* RNAi in bGRNs with *Gr89a-Gal4*(32) did not produce any difference compared to controls (Fig. 5B). In *Ih*$^{MI03196\text{-}TG4.0}$ (*Ih-TG4.0*) flies, the protein trap *T2A-Gal4* is inserted into one of the *Ih* introns, resulting in reliable spatiotemporal reporting of *Ih* expression(55,56). In response to NMM, the i-type bristles of animals expressing *TrpA1(B)* under the control of *Ih-TG4.0* produced short spikes resembling sucrose-induced sGRN spikes and larger bGRN spikes resulting from native TRPA1 expression (36). This suggests *Ih* is expressed in sGRNs (Fig. 5C,D) because i-type bristles contain only two GRNs. Previously, we reported that the dominant negative variant of TRPA1(A) {TRPA1(A)dn} dramatically attenuated phototoxin taste responses in bGRNs (*31*). Driving TRPA1(A)dn with *Ih-TG4.0* did not significantly reduce responses to the NMM-aided phototoxin riboflavin, indicating little if any *Ih-TG4.0* expression in bGRNs (Fig. 5E,F). Moreover, driving the expression of Kir2.1 with *Ih-TG4.0* produced a minimal reduction of the bGRN response to caffeine compared to the *Gal4*-only control and a dramatic reduction in sucrose-evoked firing (Fig. 5G,H). These data are consistent with a much higher expression of *Ih-TG4.0* in sGRNs than in bGRNs. According to the results of our GRN-specific *Ih* RNAi and reporter analyses, HCN expression in sGRNs is critical for counteracting the hyperpolarization putatively induced by bGRN excitation, leading to unilateral ephaptic inhibition.

Ectopic expression of Ih in bGRNs confers resistance to sGRN excitation-dependent ephaptic inhibition.

Since HCN expression in sGRNs is necessary for unilateral inhibition, we next examined the effect of HCN misexpression in bGRNs. After generating transgenic *UAS-Ih-RF* flies (51), we drove HCN expression in WT sGRNs using *Gr64f-Gal4.* The recordings of these *Ih-RF*-expressing sGRNs were indistinguishable from those of the control genotypes, indicating no effect on directionality (Fig. 5I). On the other hand, ectopic expression of *Ih-RF* in bGRNs using *Gr89a-Gal4* significantly attenuated sGRN excitation-dependent bGRN inhibition (Fig. 5J top, fig. S6). This was in contrast with the bilaterality we observed in *Ih*-deficient GRNs (Fig. 4 and 5A), indicating that the *Ih* cDNA endows GRNs with resilience to ephaptic inhibition. In addition, *Ih* misexpression permitted sGRN inhibition upon optogenetic bGRN excitation (Fig. 5J bottom), indicating that *Ih* can reverse the direction of ephaptic inhibition as well as help GRNs resist the inhibition. Thus, multiple lines of evidence have converged to indicate that differential HCN expression in GRNs determines the directionality of ephaptic inhibition.

Chemosensory excitation of s- and bGRNs confirms the requirement of Ih expressed in sGRNs for unilateral interaction.

We next sought to confirm our optogenetic findings by testing tastant-driven inhibition. Knock down of *Ih* in sGRNs, but not bGRNs, appeared to reverse the direction of ephaptic inhibition (Fig. 6A,B), as we observed with Ih^{f03355} (Fig. 4A,B). Expression of *Ih-RF* in sGRNs, but not bGRNs, rescued Ih^{f03355} (Fig. 6C,D), confirming that HCN acts in sGRNs to unilateralize the inhibition. Consistent with our optogenetic results with *Ih-RF* misexpression in WT bGRNs, we found chemically stimulated GRNs misexpressing *Ih-RF* also showed inverted lateral inhibition (Fig. 6E,F). Thus, our experiments with chemical stimulation were consistent with our optogenetic results.

Bilateral GRN interactions resulting from Ih deficiency in sGRNs impair the discernment of bitter-laced sucrose.

We next examined the significance of the unilateral inhibition in feeding using a CAFE assay designed to assess sucrose preference (Fig. 6I). To compare the unilaterality of WT with the bilateral GRN interactions of *Ih* mutants, we offered flies a choice between a sucrose (30 mM) solution with caffeine (10 mM) and a caffeine-only (10 mM) solution (Fig. 6J). Remarkably, while WT were strongly attracted to the sucrose-caffeine solution, Ih^{f03355} and *Ih-TG4.0/+* were not (Fig. 6J). The defects introduced by both alleles were rescued by the *Ih*-containing genomic fragment {*Ih*}. We found *Ih* expression in sGRNs was necessary to achieve high preference indices, as both *Ih* RNAi knock down and *Ih* cDNA rescue in sGRNs, but not bGRNs, differed significantly from their respective controls (Fig. 6K,L). Although *Ih* misexpression in bGRNs reversed the lateral interaction between the GRNs (Fig. 5J and 6E,F), we still observed a feeding defect when we adjusted the concentrations of caffeine and sucrose toward a balance of increased bitterness (Fig. 6M,N). This was probably due to a shift in the balance of the GRN interaction in a way that was distinct from that of *Ih*-deficient flies. In addition to the unidirectionalized GRN interaction that occurs when *Ih-RF* is misexpressed in bGRNs, the spiking of sGRNs in response to the caffeine/sucrose mixture was not different from control genotypes (Fig. 6E,F). In contrast, *Ih*-deficient sGRNs showed a significant reduction (Fig. 6B,D, bottom gray-filled box plots labeled with "Mix."). These results suggest the *Ih*-dependent unilateral GRN interaction is required for *Drosophila* to readily ingest sweets mixed with bitter chemicals.

Ih expressed in sGRNs promotes bGRN activity while also limiting sGRN excitability.

We noticed unexpected changes in GRN spiking responses to single tastants in some genotypes. In addition to unilateral inhibition, both Ih^{f03355} (Fig. 4A,B) and sGRN-specific *Ih* knock down (Fig. 6A,B) showed significant decreases in bGRN spiking in response to bitter-only stimulation compared to control genotypes (‡: Dunn's, $p < 0.05$). This suggests HCN expressed in sGRNs may potentiate bGRNs. We also found that *{Ih}* and sGRN-specific expression of *Ih-RF* rescued the bGRN suppression observed in these genotypes (Fig. 6C,D, ‡‡: Dunn's, $p < 0.01$ between genotypes). Moreover, ectopic expression of *Ih-RF* in bGRNs increased sucrose-induced sGRN firing (Fig. 6E,F, ‡‡: Dunn's, $p < 0.01$ between genotypes), similar to our observation that HCN expression in sGRNs was necessary for normal bGRN sensitivity. These data suggest HCN expression in a specific GRN upregulates the activity of that cell's neighboring GRN. On the other hand, ectopic expression of *Ih-RF* in bGRNs reduced bGRN firing in response to a caffeine-sorbitol solution compared to control genotypes (Fig. 6E,F, ‡: Dunn's, $p < 0.05$). This suggests HCN expression suppresses neurons. In bGRNs misexpressing HCN, we found that HCN expression repressed bGRN responses to relatively high caffeine concentrations, such as 2 mM and 10 mM, flattening the caffeine dose response curve (Fig. 6G). This result suggests robust excitation of bGRNs is limited by HCN expression. In sGRNs overexpressing HCN, however, only prolonged sGRN firing was significantly reduced 5 sec after initial contact with sucrose, possibly because sGRNs express some innate level of HCN (Fig. 6H). We also found sGRN-specific *Ih* RNAi increased sGRN responses to sucrose-only stimulation, implying that native HCN expression in sGRNs is required to restrict sGRN activity (Fig. 6A,B, §: Games-Howell test, $p < 0.05$ between genotypes). We did not see increased sGRN responses to sucrose associated with *Ih* loss-of-function alleles (Fig. 4A,B and 6C,D), possibly because broad *Ih* expression in the brain can set the sensitivity of the GRN circuits remotely (57).

Meanwhile, we found interesting genetic interactions in bGRN responses triggered by bitter-only stimulation. The bGRN responses to various bitters in labellar gustatory bristle sensilla were increased in *Gr64af* compared to WT (Fig. 7A, fig. S7A). We observed a similar bGRN sensitization with sGRN-specific Kir2.1 expression to inhibit sGRN firing but not with TNT expression to block sGRN chemical synaptic transmission (Fig. 7B,C). Together with the *Gr64af* data, this suggests sGRN excitability regulates bGRNs. When we combined the sGRN-hindering genotypes with the *Ih* alleles Ih^{f03355} or *Ih-TG4.0,* we found that the sGRN inhibition-induced increase in bGRN activity could be relieved by disruptions in the *Ih* gene (Fig. 7B,D). This suggests *Ih* gene expression upregulates bGRNs, as do genetic changes like *Gr64af* and *Gr5a>Kir2.1*. Note that *Ih-TG4.0* is homozygous lethal but dominant in the unilateral programming phenotype, as *Ih-TG4.0* heterozygotes showed a reversal of the lateral inhibition in extracellular recordings (fig. S7B). Since HCN is expressed in sGRNs that inhibit bGRNs, HCN-dependent bGRN upregulation may relate to our observation that HCN limits sGRN excitation (Fig. 6).

Sensillum potential mediates intercellular Ih-dependent bGRN regulation but does not affect the direction of unilateral inhibition.

How, then, does the HCN-dependent restriction on sGRN excitability lead to increased bGRN sensitivity? As in several other sensory organs, insect taste sensilla are sensitized as they employ active transport to create a positive sensillum potential (SP), which is a form of transepithelial potential (TEP), across the GRNs and their supporting cells between the sensillum lymph and the hemolymph (12,58–60). Receptor-mediated inward currents flowing into sensory neurons can lower this SP, which may hyperpolarize other neurons that share the same sensillum

lymph (12,60). Based on this, we postulated that HCN might preserve the SP by limiting sGRN excitability, thereby maintaining bGRN sensitivity. Typically, we performed extracellular recordings on flies 4-5 days after eclosion, before which they were kept in a vial with fresh regular cornmeal food containing 400 mM D-glucose. Under our hypothesis, such a sweet environment would lower the SP and bGRN sensitivity more in *Ih* mutants than in WT, as HCN limits sGRN excitability. To test this possibility, we fed WT and Ih^{f03355} flies overnight with either non-sweet sorbitol alone (200 mM) or a sweet mixture of sorbitol (200 mM) + sucrose (100 mM). Although sorbitol is not sweet, it is a digestible sugar that provides *Drosophila* with calories (33). We found the sweet sucrose medium significantly reduced caffeine-induced bGRN responses in both genotypes compared to the sorbitol only medium, but Ih^{f03355} bGRN spike frequencies were decreased even more compared to WT (Fig. 7E). This suggests the reduced bGRN activity in the mutants correlates with long-term sGRN excitation. We next measured SP in the absence of taste stimulation as the net potential difference between the sensillum and the labellum. We calculated net potential difference by subtracting the DC offset (61) from the raw potential difference (fig. S7C). DC offsets (also known as DC biases) measured from various parts of the body were indistinguishable, indicating that DC offsets are largely invariable across an individual fly (fig. S7D,E). We found that we could reduce apparent SP by deflecting the bristle sensillum by 45º (fig. S7F-H), activating the sensillum's mechanosensory neuron. When we did the same experiment with $nompC^{f00642}$, a loss-of-function allele of *nompC,* which encodes a mechanosensory TRPN channel(62), this reduction in SP disappeared (fig. S7E,F). Like the bGRN response (Fig. 7E), the SP reduction induced by sweet medium was more dramatic in HCN-deficient animals than in WT (Fig. 7F), indicating a close relationship between bGRN activity and SP. When we maintained the flies on regular cornmeal food, Ih^{f03355} and *Ih-TG4.0/+* showed a lower SP than WT (Fig. 7G), as observed with the sucrose medium (Fig. 7F). Similar to the bGRN spiking response to bitter-only stimulation (Fig. 7A,D, fig. S7A), the SP of i-bristles in *Gr64af* flies was increased, returning again to WT levels when combined with Ih^{f03355} and *Ih-TG4.0/+* (Fig. 7G). This confirms the intimate relationship between bGRN sensitivity and SP. To determine whether HCN expression in GRNs governs SP, we introduced *Ih-RF* into the bGRNs or sGRNs of Ih^{f03355}. We then found that HCN expression in either type of GRN significantly increased SP (Fig. 7H). Notably, *Ih* rescue in sGRNs was more effective in raising SP than in the ectopic bGRNs, suggesting that limiting sGRN responses is key to preserving SP in sweet overripe fruits that are the natural feeding niche of fruit flies (63). Misexpression of *Ih-RF* in bGRNs in WT also elevated SP compared to controls (Fig. 7I). This SP increase is consistent with our observation that HCN misexpression increased sGRN spiking (Fig. 6E,F) and it supports the hypothesis that HCN controls the activities of neighboring GRNs via SP. We speculate that the increase in SP induced by HCN misexpression in bGRNs would not increase bGRN activity because HCN suppresses robust firing in the neurons that express it (Fig. 6G). We used sorbitol media to determine whether the interaction between GRNs would be shifted in the absence of sweet stimuli. Unlike Ih^{f03355} flies maintained on the regular sweet cornmeal medium (Fig. 4A,B) or on the sucrose medium (Fig. 7E and 7J, right), those on the non-sweet sorbitol medium exhibited caffeine-induced bGRN responses (without sucrose) comparable to those of WT (Fig. 7J, left, open boxes). On the other hand, the HCN-dependent sweetness dominance persisted regardless of food sweetness (Fig. 7J,K), indicating that SP regulates GRN sensitivity but not the direction of the lateral inhibition.

To determine the behavioral implications of HCN-assisted SP preservation, we subjected flies exposed to long-term sweetness while being maintained on regular sweet cornmeal diet to a CAFE with a choice of water or 4 mM caffeine solution. Indicative of reduced bitter sensitivity, Ih^{f03355} showed significantly reduced 4 mM caffeine avoidance than WT (Fig. 7L). In contrast,

when we isolated the flies from sweet food for 20 hrs, both WT and *Ih*^{f03355} showed similar bitter avoidance. Thus, the unilateral coding for the interaction between sweetness and bitterness is critical for flies to detect bitter-buried sugars and maintain bitter sensitivity. This ensures they will ingest bitter-laced carbohydrates but also avoid the same toxic substance in the absence of any caloric value.

Discussion

We report that *Ih* plays two opposing roles in the ephaptic coding of sweet-bitter interactions. HCN stabilizes the membrane potential because the HCN current (also known as I_h) is activated by hyperpolarization and conducts cations. In doing so, it counters both hyperpolarization and depolarization (64). A population of HCN channels stays open at resting membrane potentials, but is closed by depolarization. This channel closing reduces cation conductance through HCN, providing resistance to further depolarization. This characteristic of I_h is conserved in *Drosophila*, as *Drosophila* HCN is also activated by hyperpolarization (49). Because of HCN's unique electrophysiological properties, the membrane potential of HCN-expressing sGRNs is likely stabilized at rest, conferring sGRNs with resistance to both inhibition and overexcitation. The former leads to unilateral inhibition, while the latter preserves SP and GRN sensitivity (Fig. 7M).

Unilateral ephaptic coding achieves both carbohydrate prioritization and sensitive bitterness detection.

The unilaterality of gustatory ephaptic inhibition allows peripheral GRNs to act as a unique information processing device, achieving signal dominance through the rectification of lateral inhibition against the cell size gradient. On the other hand, bilaterality allows two different stimuli to cancel each other with fine tuning achieved via cell size-dependent asymmetry of their mutual inhibition (12). This may allow for the integration of input valence (13,65). It is interesting that GRNs have opted for a genetic reprogramming of ephaptic inhibition by means of the *Ih* gene, rather than having large sGRNs and small bGRNs as in the olfactory system. It is possible that a larger cell size is critical for bGRNs in detecting and avoiding bitter toxins, whereas bGRNs also need to be controlled by sGRNs to readily secure sufficient energy for basic metabolism. Neuronal process diameter generally shows a positive correlation with soma size (66–69). Thick dendrites may enable bGRNs to expose more bitter receptor molecules to the environment, lowering the bitter detection threshold. In addition, large axon diameters are often associated with higher rates of action potential propagation (69,70) and larger synaptic boutons (71), suggesting that soma size largely determines the rate of intraneuronal signal propagation and synaptic transmission robustness. Therefore, bGRNs may be larger because of the animal's evolutionary need to sensitively detect and rapidly respond to gustatory information regarding the presence of potential toxins. The *Ih*-dependent preservation of bGRN activity via SP we discovered is consistent with such evolutionary pressure to maintain sensitive bGRN function, despite the contrasting role of *Ih* in the unilateralization of ephaptic coupling that enhances bGRN inhibition. Thus, the adoption of *Ih* for the programming of GRN interactions allows flies to take advantage of the large size of bGRNs while also facilitating the detection of sugars mixed with bitter chemicals. Given the ecological niche of the flies, the importance of detecting and ingesting sugars co-presented with bitters may have evolutionarily forced unilateral inhibition on GRN interactions. Beyond insects, herbivory is widely practiced, suggesting that sweetness dominance must be common. Indeed, even humans showed reduced perception of taste modalities co-offered with sweetness (22–29). It will be intriguing to learn in future studies how humans and other animals promote sweetness dominance.

Potential implications in other contexts

Here, we have uncovered a novel, genetically controlled information processing mechanism, a miniature circuit encoding sweetness dominance comprised only of peripheral receptor neurons. We suspect similar principles are widespread, given the ubiquity of ephaptic coupling in the brain and the prevalence of compartmentalized cells across the animal kingdom (13). Mammalian taste cells, which are capable of entraining action potentials (72,73), are compartmentalized in taste buds. This suggests ephaptic inhibition may also underly peripheral coding of mammalian gustatory interactions. In addition, it is possible that HCN modulates ephaptic interactions in other common neuronal interfaces (6,74) beyond the specialized sites of ephaptic coupling like the axon cap and pinceau. Ephaptic coupling and HCN reportedly contribute to neural oscillations (4–7,63,74,75) in which they may cooperate to synchronize neuronal activities and generate specific wave frequencies. To date, it has been difficult to positively identify examples of ephaptic signaling because of a lack of genetic factors. But since *Ih* is associated with target neuron hyperpolarization (3) and provides GRNs with resilience to ephaptic inhibition, *Ih* may become a useful genetic tool in the discovery of other examples of ephaptic inhibition. Thus, together, our results reveal a genetic factor that is key to the directional control of ephaptic inhibition and that is physiologically important. We expect these results will accelerate future research in the field of ephaptic coupling.

References

1. Katz B, Schmitt OH. Electric interaction between two adjacent nerve fibres. J Physiol. 1940 Feb 2;97(4):471.
2. Anastassiou CA, Koch C. Ephaptic coupling to endogenous electric field activity: Why bother? Vol. 31, Current Opinion in Neurobiology. Elsevier Ltd; 2015. p. 95–103.
3. Van der Goes van Naters W. Inhibition among olfactory receptor neurons. Front Hum Neurosci [Internet]. 2013 Oct 23 [cited 2022 Nov 9];7(OCT). Available from: https://pubmed.ncbi.nlm.nih.gov/24167484/
4. Han KS, Guo C, Chen CH, Witter L, Osorno T, Regehr WG. Ephaptic Coupling Promotes Synchronous Firing of Cerebellar Purkinje Cells. Neuron [Internet]. 2018 Nov 7 [cited 2021 May 13];100(3):564-578.e3. Available from: https://pubmed.ncbi.nlm.nih.gov/30293822/
5. Chiang CC, Shivacharan RS, Wei X, Gonzalez-Reyes LE, Durand DM. Slow periodic activity in the longitudinal hippocampal slice can self-propagate non-synaptically by a mechanism consistent with ephaptic coupling. Journal of Physiology [Internet]. 2019 Jan 1 [cited 2021 May 13];597(1):249–69. Available from: https://pubmed.ncbi.nlm.nih.gov/30295923/
6. Anastassiou CA, Perin R, Markram H, Koch C. Ephaptic coupling of cortical neurons. Nat Neurosci [Internet]. 2011 Feb [cited 2022 Nov 9];14(2):217–24. Available from: https://pubmed.ncbi.nlm.nih.gov/21240273/
7. Subramanian M, Chiang CC, Couturier NH, Durand DM. Theta waves, neural spikes and seizures can propagate by ephaptic coupling in vivo. Exp Neurol. 2022 Aug 1;354:114109.
8. Stacey RG, Hilbert L, Quail T. Computational study of synchrony in fields and microclusters of ephaptically coupled neurons. J Neurophysiol. 2015 May 1;113(9):3229.
9. Blot A, Barbour B. Ultra-rapid axon-axon ephaptic inhibition of cerebellar Purkinje cells by the pinceau. Nature Neuroscience 2014 17:2. 2014 Jan 12;17(2):289–95.
10. Furukawa T, Furshpan EJ. Two inhibitory mechanisms in the Mauthner neurons of goldfish. J Neurophysiol. 1963 Jan 1;26:140–76.
11. Su CY, Menuz K, Reisert J, Carlson JR. Non-synaptic inhibition between grouped neurons in an olfactory circuit. Nature [Internet]. 2012 Dec 12 [cited 2023 Jan 24];492(7427):66. Available from: /pmc/articles/PMC3518700/

12. Zhang Y, Tsang TK, Bushong EA, Chu LA, Chiang AS, Ellisman MH, et al. Asymmetric ephaptic inhibition between compartmentalized olfactory receptor neurons. Nat Commun [Internet]. 2019 Dec 1 [cited 2021 May 13];10(1):1–16. Available from: https://doi.org/10.1038/s41467-019-09346-z
13. Ng R, Wu ST, Su CY. Neuronal Compartmentalization: A Means to Integrate Sensory Input at the Earliest Stage of Information Processing? BioEssays [Internet]. 2020 Aug 1 [cited 2023 Feb 13];42(8):2000026. Available from: https://onlinelibrary.wiley.com/doi/full/10.1002/bies.202000026
14. Faber DS, Pereda AE. Two forms of electrical transmission between neurons. Front Mol Neurosci. 2018 Nov 21;11:427.
15. Faber DS, Korn H. A Neuronal Inhibition Mediated Electrically. Science (1979). 1973 Feb 9;179(4073):577–8.
16. Meyerhof W, Behrens M, Brockhoff A, Bufe B, Kuhn C. Human Bitter Taste Perception. Chem Senses. 2005 Jan 1;30(suppl_1):i14–5.
17. Chu B, Chui V, Mann K, Gordon MD. Presynaptic gain control drives sweet and bitter taste integration in Drosophila. Current Biology [Internet]. 2014 Sep 8 [cited 2020 Sep 4];24(17):1978–84. Available from: https://pubmed.ncbi.nlm.nih.gov/25131672/
18. Sarah French A, Sellier MJ, Agha Moutaz A, Guigue A, Chabaud MA, Reeb PD, et al. Dual mechanism for bitter avoidance in Drosophila. J Neurosci [Internet]. 2015 [cited 2023 Aug 4];35(9):3990–4004. Available from: https://pubmed.ncbi.nlm.nih.gov/25740527/
19. Chen Y, Amrein H. Enhancing Perception of Contaminated Food through Acid-Mediated Modulation of Taste Neuron Responses. Current Biology. 2014 Sep 8;24(17):1969–77.
20. Charlu S, Wisotsky Z, Medina A, Dahanukar A. Acid sensing by sweet and bitter taste neurons in Drosophila melanogaster. Nat Commun [Internet]. 2013 Jan [cited 2014 Jan 22];4(May):2042. Available from: http://www.pubmedcentral.nih.gov/articlerender.fcgi?artid=3710667&tool=pmcentrez&rendertype=abstract
21. Jeong YT, Shim J, Oh SR, Yoon HI, Kim CH, Moon SJ, et al. An Odorant Binding Protein required for suppression of sweet taste by bitter chemicals. Neuron [Internet]. 2013 Aug 8 [cited 2023 Jan 25];79(4):725. Available from: /pmc/articles/PMC3753695/
22. Keast RSJ, Breslin PAS. An overview of binary taste-taste interactions. Food Qual Prefer. 2003 Mar 1;14(2):111–24.
23. Green BG, Lim J, Osterhoff F, Blacher K, Nachtigal D. Taste mixture interactions: Suppression, additivity, and the predominance of sweetness. Physiol Behav [Internet]. 2010 Dec 2 [cited 2021 May 13];101(5):731–7. Available from: /pmc/articles/PMC2975745/
24. Calvino AM, García-Medina MR, Cometto-muniz JE. Interactions in caffeine–sucrose and coffee–sucrose mixtures: evidence of taste and flavor suppression. Chem Senses [Internet]. 1990 Nov 1 [cited 2023 Jan 25];15(5):505–19. Available from: https://academic.oup.com/chemse/article/15/5/505/411797
25. Pangborn RM. Taste Interrelationships. J Food Sci [Internet]. 1962 Sep 1 [cited 2023 Jan 25];27(5):495–500. Available from: https://onlinelibrary.wiley.com/doi/full/10.1111/j.1365-2621.1962.tb00133.x
26. Kamen JM, Pilgrim FJ, Gutman NJ, Kroll BJ. Interactions of suprathereshold taste stimuli. J Exp Psychol [Internet]. 1961 Oct [cited 2023 Jan 25];62(4):348–56. Available from: /record/1963-00255-001
27. Kroeze JHA, Bartoshuk LM. Bitterness suppression as revealed by split-tongue taste stimulation in humans. Physiol Behav. 1985 Nov 1;35(5):779–83.
28. Prescott J, Ripandelli N, Wakeling I. Binary Taste Mixture Interactions in PROP Non-tasters, Medium-tasters and Super-tasters. Chem Senses [Internet]. 2001 Oct 1 [cited 2023 Jan 25];26(8):993–1003. Available from: https://academic.oup.com/chemse/article/26/8/993/327689
29. Schiffman SS, Gatlin LA, Sattely-Miller EA, Graham BG, Heiman SA, Stagner WC, et al. The effect of sweeteners on bitter taste in young and elderly subjects. Brain Res Bull. 1994 Jan 1;35(3):189–204.
30. Tanimura T, Hiroi M, Inoshita T, Marion-Poll F. Neurophysiology of gustatory receptor neurones in Drosophila. SEB Exp Biol Ser. 2009 Jan;63:59–76.

31. Meunier N, Rospars J pierre, Tanimura T, Marion-Poll F. Peripheral coding of bitter taste in Drosophila. J Neurobiol. 2003 Aug;56(2):139–52.
32. Weiss LA, Dahanukar A, Kwon JY, Banerjee D, Carlson JR. The molecular and cellular basis of bitter taste in Drosophila. Neuron [Internet]. 2011 Jan 27 [cited 2012 Jul 20];69(2):258–72. Available from: http://www.pubmedcentral.nih.gov/articlerender.fcgi?artid=3033050&tool=pmcentrez&rendertype=abstract
33. Fujita M, Tanimura T. Drosophila Evaluates and Learns the Nutritional Value of Sugars. Current Biology. 2011 May 10;21(9):751–5.
34. Kim H, Kim H, Kwon JY, Seo JT, Shin DM, Moon SJ. Drosophila Gr64e mediates fatty acid sensing via the phospholipase C pathway. PLoS Genet [Internet]. 2018 Feb 1 [cited 2023 Jan 26];14(2). Available from: https://pubmed.ncbi.nlm.nih.gov/29420533/
35. Ja WW, Carvalho GB, Mak EM, de la Rosa NN, Fang AY, Liong JC, et al. Prandiology of Drosophila and the CAFE assay. Proc Natl Acad Sci U S A. 2007 May 15;104(20):8253–6.
36. Du EJ, Ahn TJ, Sung H, Jo HJ, Kim HWW, Kim STT, et al. Analysis of phototoxin taste closely correlates nucleophilicity to type 1 phototoxicity. Proc Natl Acad Sci U S A [Internet]. 2019 May 28 [cited 2019 May 28];116(24):12013–8. Available from: http://www.pnas.org/lookup/doi/10.1073/pnas.1905998116
37. Wang Z, Singhvi A, Kong P, Scott K. Taste representations in the Drosophila brain. Cell [Internet]. 2004 Jun 25;117(7):981–91. Available from: http://www.ncbi.nlm.nih.gov/pubmed/15210117
38. Baines RA, Uhler JP, Thompson A, Sweeney ST, Bate M. Altered electrical properties in Drosophila neurons developing without synaptic transmission. J Neurosci [Internet]. 2001 Mar 1 [cited 2023 Jan 26];21(5):1523–31. Available from: https://pubmed.ncbi.nlm.nih.gov/11222642/
39. McGuire SE, Le PT, Osborn AJ, Matsumoto K, Davis RL. Spatiotemporal Rescue of Memory Dysfunction in Drosophila. Science (1979) [Internet]. 2003 Dec 6 [cited 2023 Jan 26];302(5651):1765–8. Available from: https://www.science.org/doi/10.1126/science.1089035
40. Broadie K, Prokop A, Bellen HJ, O'Kane CJ, Schulze KL, Sweeney ST. Syntaxin and synaptobrevin function downstream of vesicle docking in drosophila. Neuron. 1995 Sep 1;15(3):663–73.
41. Ffrench-Constant RH, Rocheleau TA, Steichen JC, Chalmers AE. A point mutation in a Drosophila GABA receptor confers insecticide resistance. Nature 1993 363:6428 [Internet]. 1993 [cited 2023 Feb 28];363(6428):449–51. Available from: https://www.nature.com/articles/363449a0
42. Liu WW, Wilson RI. Glutamate is an inhibitory neurotransmitter in the Drosophila olfactory system. Proc Natl Acad Sci U S A [Internet]. 2013 Jun 18 [cited 2023 Feb 28];110(25):10294–9. Available from: https://pubmed.ncbi.nlm.nih.gov/23729809/
43. Ammer G, Vieira RM, Fendl S, Borst A. Anatomical distribution and functional roles of electrical synapses in Drosophila. Curr Biol [Internet]. 2022 May 9 [cited 2023 Feb 28];32(9):2022-2036.e4. Available from: https://pubmed.ncbi.nlm.nih.gov/35385694/
44. Inagaki HK, Jung Y, Hoopfer ED, Wong AM, Mishra N, Lin JY, et al. Optogenetic control of Drosophila using a red-shifted channelrhodopsin reveals experience-dependent influences on courtship. Nature Methods 2013 11:3 [Internet]. 2013 Dec 22 [cited 2023 Jan 27];11(3):325–32. Available from: https://www.nature.com/articles/nmeth.2765
45. Gonzales CN, McKaughan Q, Bushong EA, Cauwenberghs K, Ng R, Madany M, et al. Systematic morphological and morphometric analysis of identified olfactory receptor neurons in Drosophila melanogaster. Elife [Internet]. 2021 Aug 1 [cited 2023 Mar 8];10. Available from: /pmc/articles/PMC8410077/
46. Rosenzweig M, Kang K, Garrity PA. Distinct TRP channels are required for warm and cool avoidance in Drosophila melanogaster. Proc Natl Acad Sci U S A [Internet]. 2008 Sep 23;105(38):14668–73. Available from: http://www.pubmedcentral.nih.gov/articlerender.fcgi?artid=2567170&tool=pmcentrez&rendertype=abstract

47. Biel M, Wahl-Schott C, Michalakis S, Zong X. Hyperpolarization-activated cation channels: from genes to function. Physiol Rev [Internet]. 2009 Jul [cited 2023 Jan 25];89(3):847–85. Available from: https://pubmed.ncbi.nlm.nih.gov/19584315/
48. Gisselmann G, Gamerschlag B, Sonnenfeld R, Marx T, Neuhaus EM, Wetzel CH, et al. Variants of the Drosophila melanogaster Ih-channel are generated by different splicing. Insect Biochem Mol Biol. 2005 May 1;35(5):505–14.
49. Fernandez-Chiappe F, Frenkel L, Colque CC, Ricciuti A, Hahm B, Cerredo K, et al. High-Frequency Neuronal Bursting is Essential for Circadian and Sleep Behaviors in Drosophila. The Journal of Neuroscience [Internet]. 2021 Jan 1 [cited 2023 Jan 29];41(4):689. Available from: /pmc/articles/PMC7842748/
50. Hu W, Wang T, Wang X, Han J. Ih Channels Control Feedback Regulation from Amacrine Cells to Photoreceptors. PLoS Biol [Internet]. 2015 Apr 1 [cited 2023 Jan 29];13(4):e1002115. Available from: https://journals.plos.org/plosbiology/article?id=10.1371/journal.pbio.1002115
51. Thistle R, Cameron P, Ghorayshi A, Dennison L, Scott K. Contact chemoreceptors mediate male-male repulsion and male-female attraction during Drosophila courtship. Cell [Internet]. 2012 May 25 [cited 2012 Jul 20];149(5):1140–51. Available from: http://www.pubmedcentral.nih.gov/articlerender.fcgi?artid=3365544&tool=pmcentrez&rendertype=abstract
52. Van Bogaert PP, Pittoors F. Use-dependent blockade of cardiac pacemaker current (If) by cilobradine and zatebradine. Eur J Pharmacol [Internet]. 2003 Oct 8 [cited 2023 Jan 30];478(2–3):161–71. Available from: https://pubmed.ncbi.nlm.nih.gov/14575801/
53. Dahanukar A, Lei YT, Kwon JY, Carlson JR. Two Gr Genes Underlie Sugar Reception in Drosophila. Neuron. 2007 Nov 8;56(3):503–16.
54. Kanca O, Zirin J, Hu Y, Tepe B, Dutta D, Lin WW, et al. An expanded toolkit for Drosophila gene tagging using synthesized homology donor constructs for CRISPR-mediated homologous recombination. Elife. 2022 Jun 1;11.
55. Lee PT, Zirin J, Kanca O, Lin WW, Schulze KL, Li-Kroeger D, et al. A gene-specific T2A-GAL4 library for drosophila. Elife. 2018 Mar 22;7.
56. Inagaki HK, Panse KM, Anderson DJ. Independent, reciprocal neuromodulatory control of sweet and bitter taste sensitivity during starvation in Drosophila. Neuron [Internet]. 2014 Nov 11 [cited 2023 Feb 7];84(4):806. Available from: /pmc/articles/PMC4365050/
57. Nin F, Hibino H, Doi K, Suzuki T, Hisa Y, Kurachi Y. The endocochlear potential depends on two K+ diffusion potentials and an electrical barrier in the stria vascularis of the inner ear. Proc Natl Acad Sci U S A [Internet]. 2008 Feb 5 [cited 2023 Jan 24];105(5):1751–6. Available from: https://www.pnas.org/doi/abs/10.1073/pnas.0711463105
58. Sollai G, Solari P, Masala C, Liscia A, Crnjar R. A K(+)/H (+) P-ATPase transport in the accessory cell membrane of the blowfly taste chemosensilla sustains the transepithelial potential. J Comp Physiol A Neuroethol Sens Neural Behav Physiol [Internet]. 2008 Nov [cited 2022 Jul 1];194(11):981–8. Available from: https://pubmed.ncbi.nlm.nih.gov/18818932/
59. Tuthill JC, Wilson RI. Mechanosensation and Adaptive Motor Control in Insects [Internet]. Vol. 26, Current Biology. Cell Press; 2016 [cited 2021 Mar 6]. p. R1022–38. Available from: /pmc/articles/PMC5120761/
60. Marion-Poll F, Van Der Pers J. Un-filtered recordings from insect taste sensilla. Entomol Exp Appl. 1996;80:113–5.
61. Sánchez-Alcañiz JA, Zappia G, Marion-Poll F, Benton R. A mechanosensory receptor required for food texture detection in Drosophila. Nature Communications 2017 8:1 [Internet]. 2017 Jan 27 [cited 2023 May 17];8(1):1–9. Available from: https://www.nature.com/articles/ncomms14192
62. Wang W, Dweck HKM, Talross GJS, Zaidi A, Gendron JM, Carlson JR. Sugar sensation and mechanosensation in the egg-laying preference shift of Drosophila suzukii. Elife. 2022;11.
63. Shah MM. Cortical HCN channels: Function, trafficking and plasticity. Journal of Physiology [Internet]. 2014 Jul 1 [cited 2021 May 13];592(13):2711–9. Available from: https://physoc.onlinelibrary.wiley.com/doi/full/10.1113/jphysiol.2013.270058

64. Wu ST, Chen JY, Martin V, Ng R, Zhang Y, Grover D, et al. Valence opponency in peripheral olfactory processing. Proceedings of the National Academy of Sciences [Internet]. 2022 Feb 1 [cited 2023 Feb 21];119(5):e2120134119. Available from: https://www.pnas.org/doi/abs/10.1073/pnas.2120134119
65. Ulfhake B, Kellerth J -O. A quantitative light microscopic study of the dendrites of cat spinal α-motoneurons after intracellular staining with horseradish peroxidase. Journal of Comparative Neurology. 1981;202(4):571–83.
66. Ulfhake B, Cullheim S. A quantitative light microscopic study of the dendrites of cat spinal gamma -motoneurons after intracellular staining with horseradish peroxidase. J Comp Neurol [Internet]. 1981 [cited 2023 Feb 13];202(4):585–96. Available from: https://pubmed.ncbi.nlm.nih.gov/7298917/
67. Lagerbäck P, Kellerth J -O. Light microscopic observations on cat Renshaw cells after intracellular staining with horseradish peroxidase. II. The cell bodies and dendrites. J Comp Neurol [Internet]. 1985 [cited 2023 Feb 13];240(4):368–76. Available from: https://pubmed.ncbi.nlm.nih.gov/3880356/
68. Westbury DR. A comparison of the structures of α- and γ-spinal motoneurones of the cat. J Physiol [Internet]. 1982 Apr 1 [cited 2023 Feb 13];325(1):79. Available from: /pmc/articles/PMC1251381/?report=abstract
69. Arbuthnott ER, Boyd IA, Kalu KU. Ultrastructural dimensions of myelinated peripheral nerve fibres in the cat and their relation to conduction velocity. J Physiol [Internet]. 1980 Nov 1 [cited 2023 Feb 13];308(1):125–57. Available from: https://pubmed.ncbi.nlm.nih.gov/7230012/
70. Innocenti GM, Caminiti R. Axon diameter relates to synaptic bouton size: structural properties define computationally different types of cortical connections in primates. Brain Struct Funct [Internet]. 2017 Apr 1 [cited 2023 Feb 13];222(3):1169–77. Available from: https://pubmed.ncbi.nlm.nih.gov/27372337/
71. Roper S. Regenerative impulses in taste cells. Science (1979). 1983;220(4603):1311–2.
72. Vandenbeuch A, Kinnamon SC. Why do taste cells generate action potentials? J Biol [Internet]. 2009 [cited 2023 Mar 2];8(4):42. Available from: /pmc/articles/PMC2688909/
73. Han KS, Chen CH, Khan MM, Guo C, Regehr WG. Climbing fiber synapses rapidly and transiently inhibit neighboring Purkinje cells via ephaptic coupling. Nat Neurosci [Internet]. 2020 Nov 1 [cited 2023 May 17];23(11):1399–409. Available from: https://pubmed.ncbi.nlm.nih.gov/32895566/
74. Pape HC. Queer current and pacemaker: the hyperpolarization-activated cation current in neurons. Annu Rev Physiol [Internet]. 1996 [cited 2023 Jan 25];58:299–327. Available from: https://pubmed.ncbi.nlm.nih.gov/8815797/
75. Lüthi A, McCormick DA. Periodicity of thalamic synchronized oscillations: the role of Ca2+-mediated upregulation of Ih. Neuron [Internet]. 1998 [cited 2023 Mar 9];20(3):553–63. Available from: https://pubmed.ncbi.nlm.nih.gov/9539128/

Acknowledgments: We would like to thank Drs. Lim, HH, Oh, WJ and Kim, G for helpful comments, and Drs. Amrein, H, Scott, K, Moon SJ, and Kwon, JY and KDRC/BDRC stock/resource centers for sharing fly lines as indicated in Methods and Materials.

Funding: National Research Foundation of Korea (NRF-2021R1A2B5B01002702, 2022M3E5E8017946 to KJK, 2021R1A2C1008418 to KhK) and Korea Brain Research Institute (23-BR-01-02, 22-BR-03-06 to KJK), funded by Ministry of Science and ICT.

Author contributions:

Conceptualization: MHL, KJK, KK

Methodology: MHL, KJK, SYK, TP, JYK

Investigation: MHL, KJK, KMJ

Visualization: MHL, KJK, SYK

Funding acquisition: KJK, KK

Project administration: JYK, KMJ

Supervision: KJK, KK, JYK, KMJ

Writing – original draft: MHL, KJK

Writing – review & editing: KK, JYK, KMJ, SYK, TP

Competing interests: Authors declare that they have no competing interests.

Data and materials availability: All data are available in the main text or the supplementary materials.

Supplementary Materials

Materials and Methods

Figs. S1 to S7

Figure 1

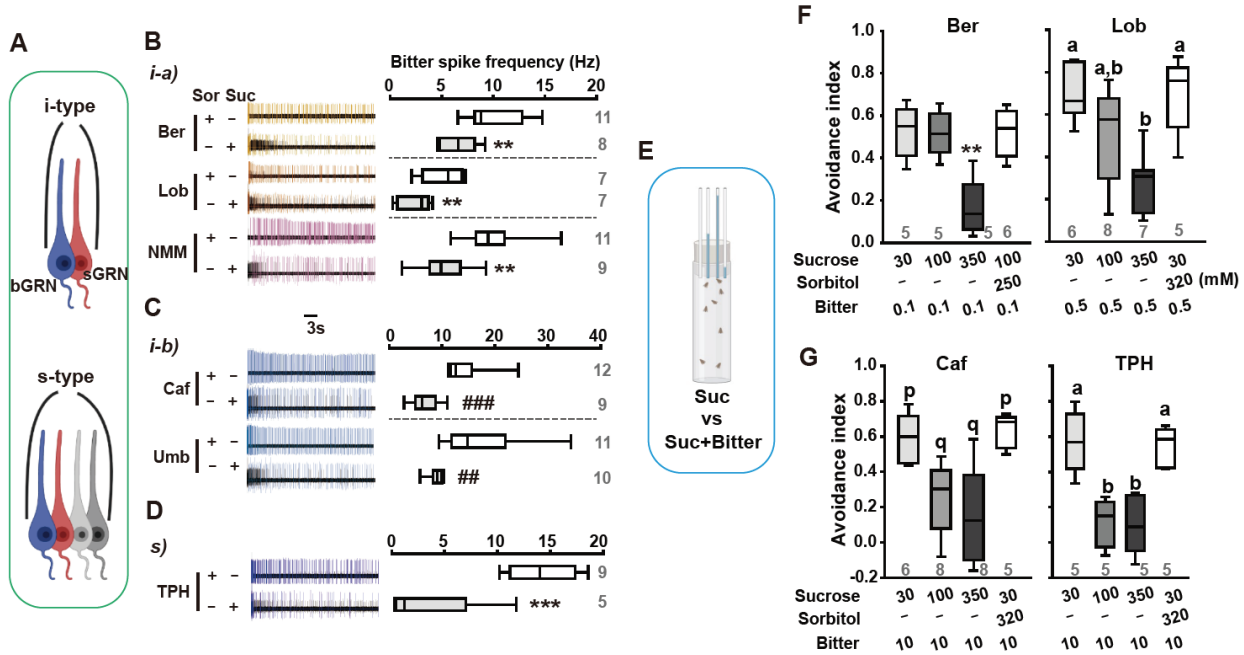

Fig. 1. Sucrose suppresses bitter-sensing GRNs and ingestion avoidance of bitters. (**A**) Schematic showing GRN organization in sensilla of the indicated bristle type in the *Drosophila* labellum. Each sensillum harbors both a bitter- and sweet-sensing GRN (bGRN and sGRN). The s-type sensilla contain water- and salt-sensing GRNs (gray) in addition to s- and bGRNs. (**B-D**) Sucrose-induced bitter suppression in i-a (B), i-b (C), and s-type (D) bristle sensilla. Spikes from sweet-sensing GRNs (sGRNs) are black, while those from bGRNs are colored (left). See also Figure S1. Box plots showing the spike frequency distributions for the first 5 sec. (**E**) Schematic showing the capillary feeder assay. (**F** and **G**) Ingestion avoidance of bitters is suppressed by sucrose. Sor: sorbitol, 50 mM; Suc: sucrose, 50 mM (Sor and Suc were 10 mM for TPH); Ber: berberine, 0.5 mM; Lob: lobeline 0.5 mM; NMM: N-methyl maleimide, 2 mM; Caf: caffeine, 2 mM; Umb: umbelliferon, 0.5 mM; TPH: theophylline, 5 mM. **, ***: Student's or Tukey's t-test, $p < 0.01$, 0.001, respectively. ##, ###: Mann-Whitney U test, $p < 0.01$, 0.001, respectively. Letters indicate statistically distinct groups (p and q: Dunn's test, and a and b: Tukey's test, $p < 0.05$). Numbers in gray indicate the number of experiments.

Figure 2

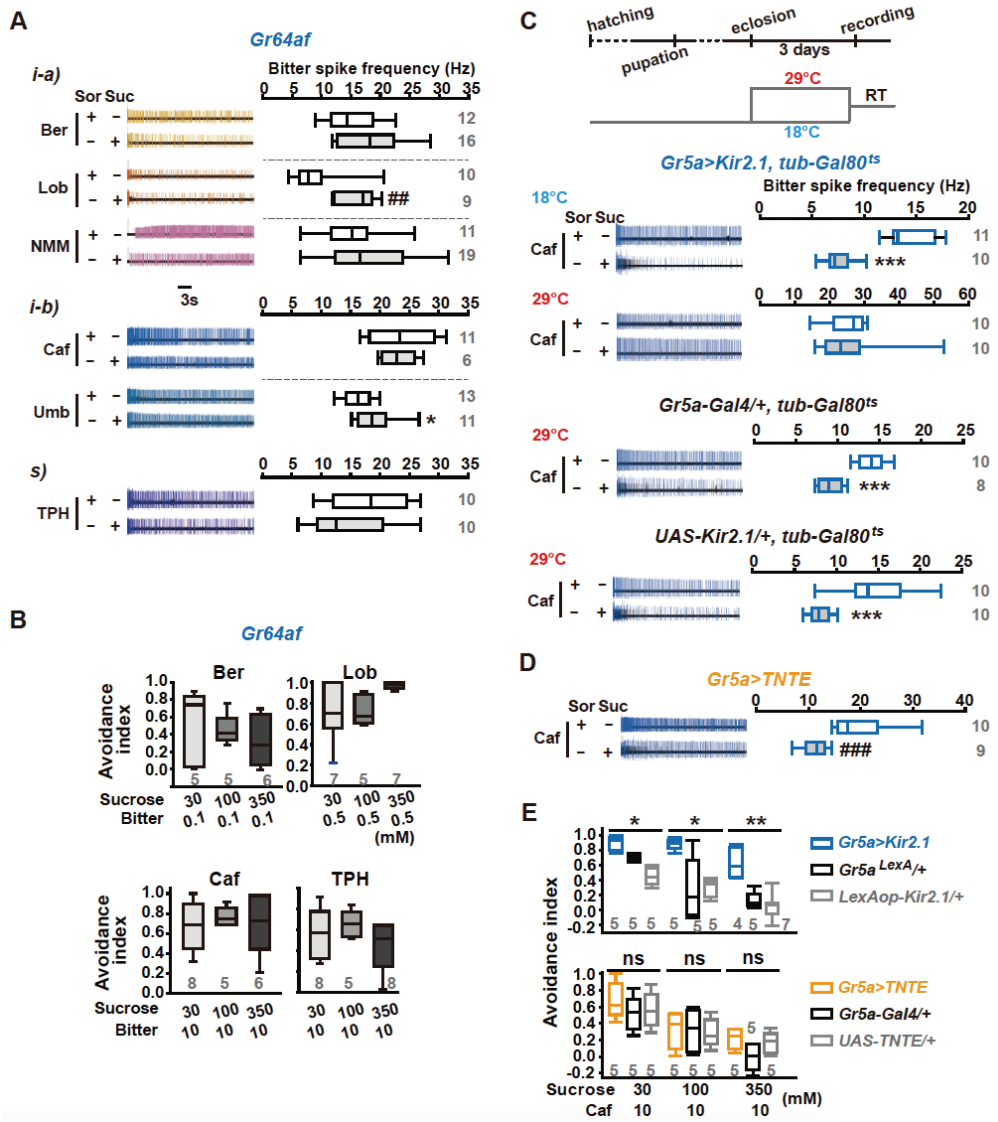

Fig. 2. Excitation of sGRNs is required for sucrose-induced bGRN inhibition. (**A**) Sucrose-induced bGRN suppression in *Gr64af* mutant flies. Typical recordings (left) and box plots (right) are shown. The same chemical concentrations used in Figure 1. (**B**) Sucrose did not suppress feeding avoidance of bitters in *Gr64af* flies. (**C**) Silencing of sGRNs abolished sucrose-dependent inhibition of bGRN caffeine responses. *Gr5a-Gal4* is expressed in sGRNs. (Top) Experimental scheme for *Gal80*^{ts} inactivation. (Bottom left) Typical recording results at the indicated temperatures. (Bottom right) Box plots from the experiments on the left. (**D**) Blocking chemical synaptic transmission with tetanus toxin light chain (TNT) did not affect sucrose-induced bGRN inhibition. (**E**) Silencing sGRNs but not blocking transmission reduced sucrose-dependent inhibition of caffeine avoidance. *, **, ***: Student's t- or Tukey's test, $p < 0.5$, 0.01, 0.001, respectively. ##, ###: Mann-Whitney U test, $p < 0.01$, 0.001, respectively. Gray numbers indicate the number of experiments.

Figure 3

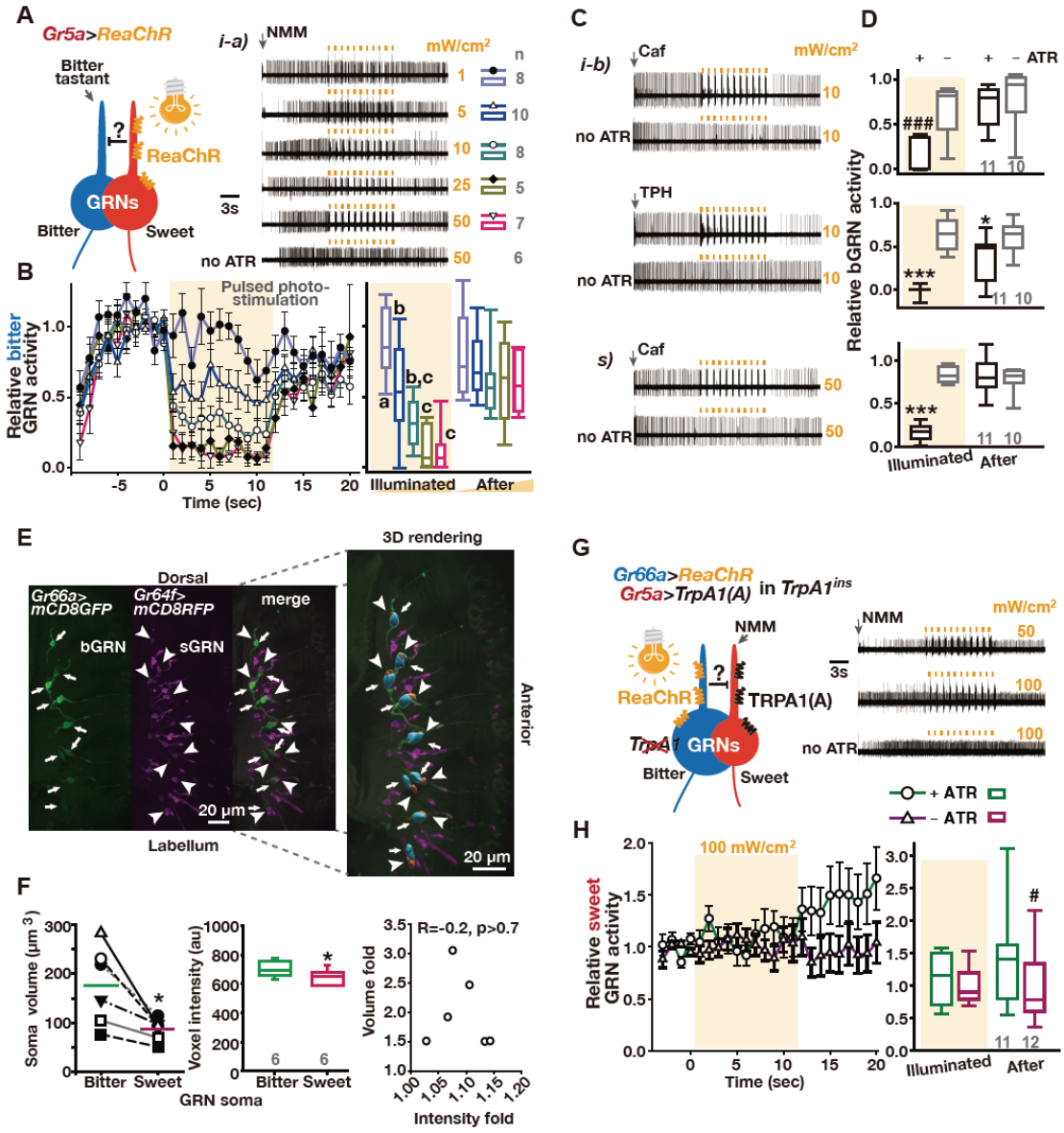

Fig. 3. Inhibition between GRNs is unilateral against the cell size gradient. (**A** and **B**) Optogenetic activation of sGRNs inhibits bGRNs activated by the TRPA1 agonist NMM (2 mM). Typical recordings showing irradiance dependence appear with a diagram illustrating the experimental design (A). ReaChR was expressed in sGRNs. 0.1-sec illuminations are indicated by small orange boxes. Average normalized spike frequencies of bGRNs for 0.9 seconds immediately after 0.1-sec illuminations at the indicated irradiance levels were plotted along the time axis (B). A translucent orange box indicates the time range over which light pulses were applied. Right, box plots showing average bGRN spiking frequencies during and after irradiation. (**C**) Typical optogenetic recordings following stimulation by the indicated bitters (Caf, 2 mM; TPH, 5 mM). (**D**) Box plots summarizing normalized data from (C). (**E**) bGRN soma volume was larger than that of its neighboring sGRN. Visualization of each GRN was achieved with the indicated membrane-tethered fluorescent proteins. 3D renderings for morphometric analyses were performed using Imaris 9.6.1. Arrows: bGRN soma. Arrowheads:

sGRN soma. (**F**) Paired comparisons of soma volumes for juxtaposed GRNs (left). *: Paired t-tests, $p < 0.05$. bGRN and sGRN soma pairs with voxel intensities < 10% different were used for the paired analyses from the left (middle). Unpaired t-tests, $p < 0.05$. Volume and voxel intensity differences showed little correlation (right). (**G**) No bGRN-dependent sGRN inhibition was observed. Experimental design with TRPA1-expressing sGRNs and ReaChR-expressing bGRNs in *TrpA1*-deficient mutants (left). Typical recording results (right, NMM, 10 mM). (**H**) Average normalized spike frequencies of sGRNs for 0.9 second immediately after a 0.1-sec illumination at the indicated level of irradiance are plotted along the time axis. Letters indicate statistically different data groups, Dunn's, $p < 0.05$ (B). *, ***: Student's t-test, $p < 0.05$, 0.001, respectively (D). #, ###: Mann-Whitney U test, $p < 0.05$, 0.001, respectively (D,H). Gray numbers are n.

Figure 4

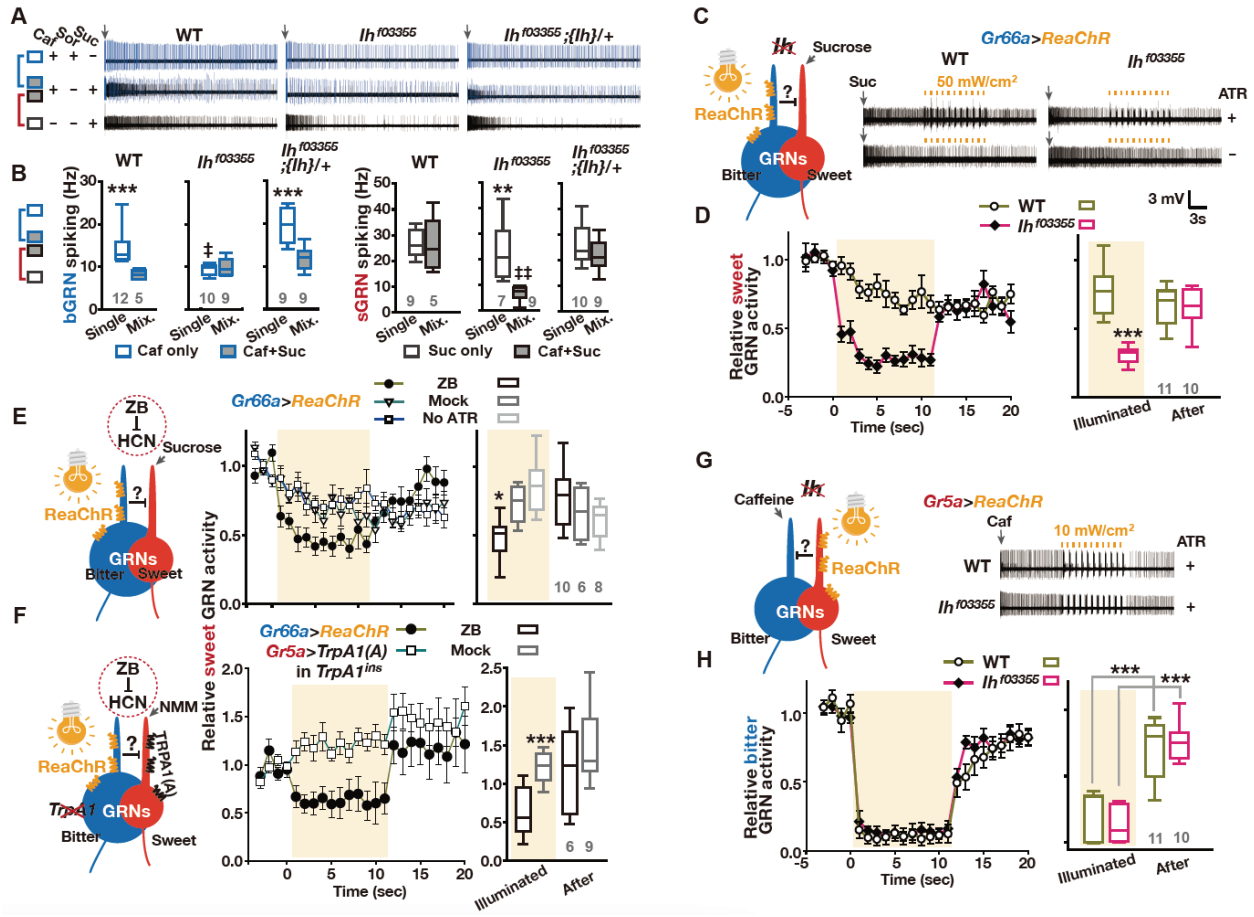

Fig. 4. HCN loss-of-function makes the normally unilateral inhibition bilateral. (**A** and **B**) Lateral inhibition in the *Ih* mutant Ih^{f03355} is reversed. Typical recordings from the indicated genotypes (A). Box plots of average spike frequencies for the first 5 sec. *{Ih}*: a genomic fragment containing the entire *Ih* locus. Sor and Suc, 50 mM; Caf, 2 mM. (**C** and **D**) Optogenetic recordings reveal that bGRN-dependent sGRN inhibition is possible in Ih^{f03355}. Suc, 10 mM. (**E** and **F**) The chemical inhibitor of HCN zatebradine (ZB) reversed the lateral inhibition in WT under optogenetic experimental settings. Suc, 10 mM; NMM, 10 mM. (**G** and **H**) sGRN-dependent bGRN inhibition was readily observed in Ih^{f03355}, indicating bilateral inhibition in the mutant. Caf, 2 mM. *, **, ***: Student's t-test between single and mixed stimulations, $p < 0.5$, 0.01, 0.001, respectively. ‡ and ‡‡: Dunn's between genotypes, $p < 0.05$ and 0.01, respectively.

Figure 5

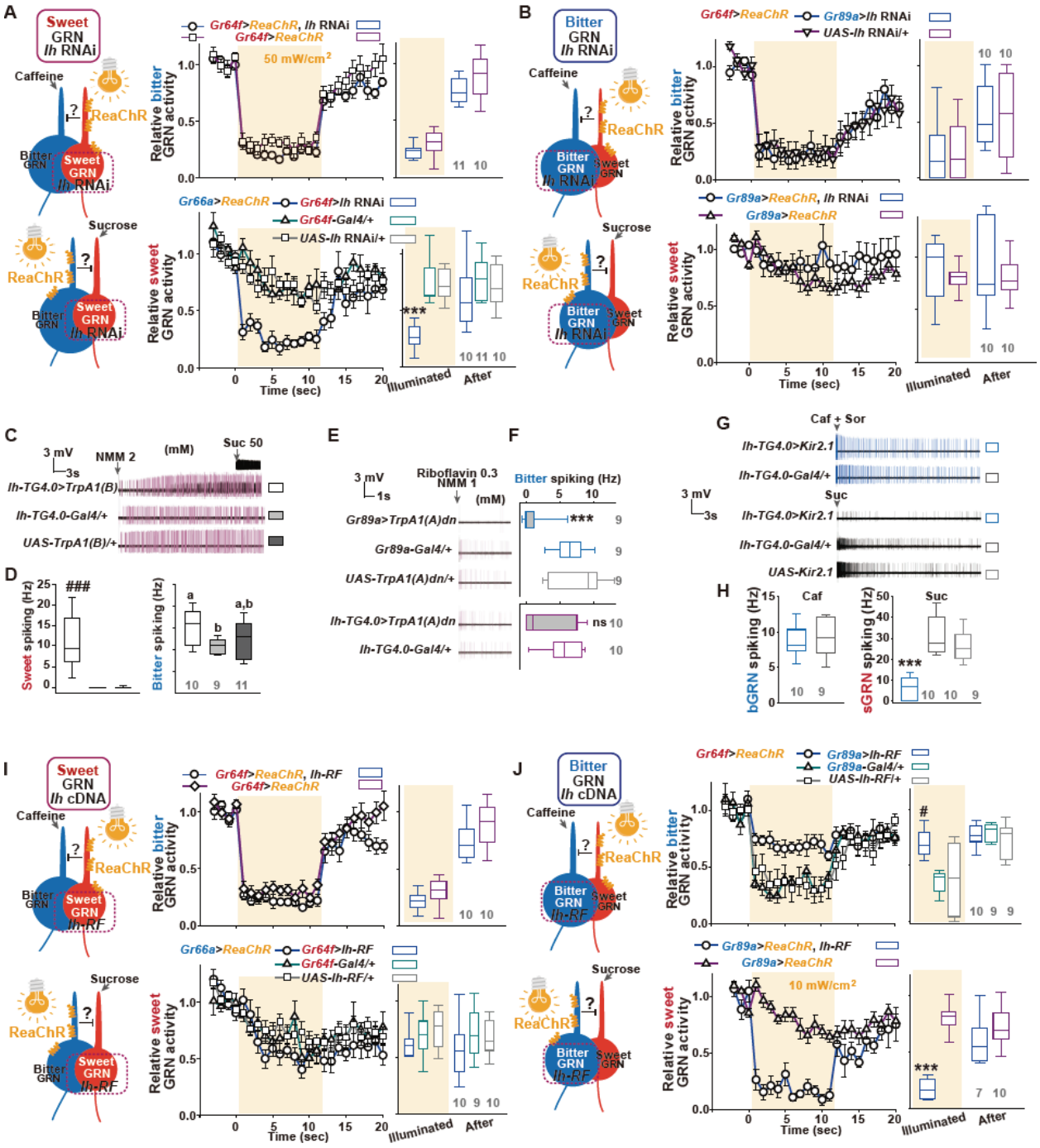

Fig. 5. HCN expressed in sGRNs is required for unilateral inhibition. (**A** and **B**) *Ih* RNAi in sGRNs made the GRN interaction bilateral. See the accompanying diagrams for each experimental design (left). (**C-H**) An *Ih* reporter was expressed more highly in sGRNs than bGRNs. When we used *Ih-TG4.0* to drive expression of TRPA1(B), we found sGRNs generate small spikes in response to NMM to accompany the large spikes of the bGRNs (C and D). In *Ih-TG4.0* flies driving TRPA1(A)dn, the response of bGRNs to riboflavin was unaffected (E and F). But *Ih-TG4.0*-driven expression of Kir2.1 dramatically reduced spiking in response to sucrose

stimuli (G and H). (**I** and **J**) Gain-of-function experiments with the *Ih-RF* cDNA raised the possibility that HCN-expressing GRNs resist lateral inhibition. See the accompanying diagrams for each experimental design (left). ***: Unpaired t- or Tukey's test, $p < 0.001$. #, ###: Dunn's, $p < 0.05$, 0.001, respectively. Letters mark statistically different groups (D): Welch's ANOVA, Games-Howell test, $p < 0.05$. NMM, 2 mM; Suc, 50 mM; Caf, 2 mM. NMM, 1 mM for the riboflavin (0.3 mM) experiments (E).

Figure 6

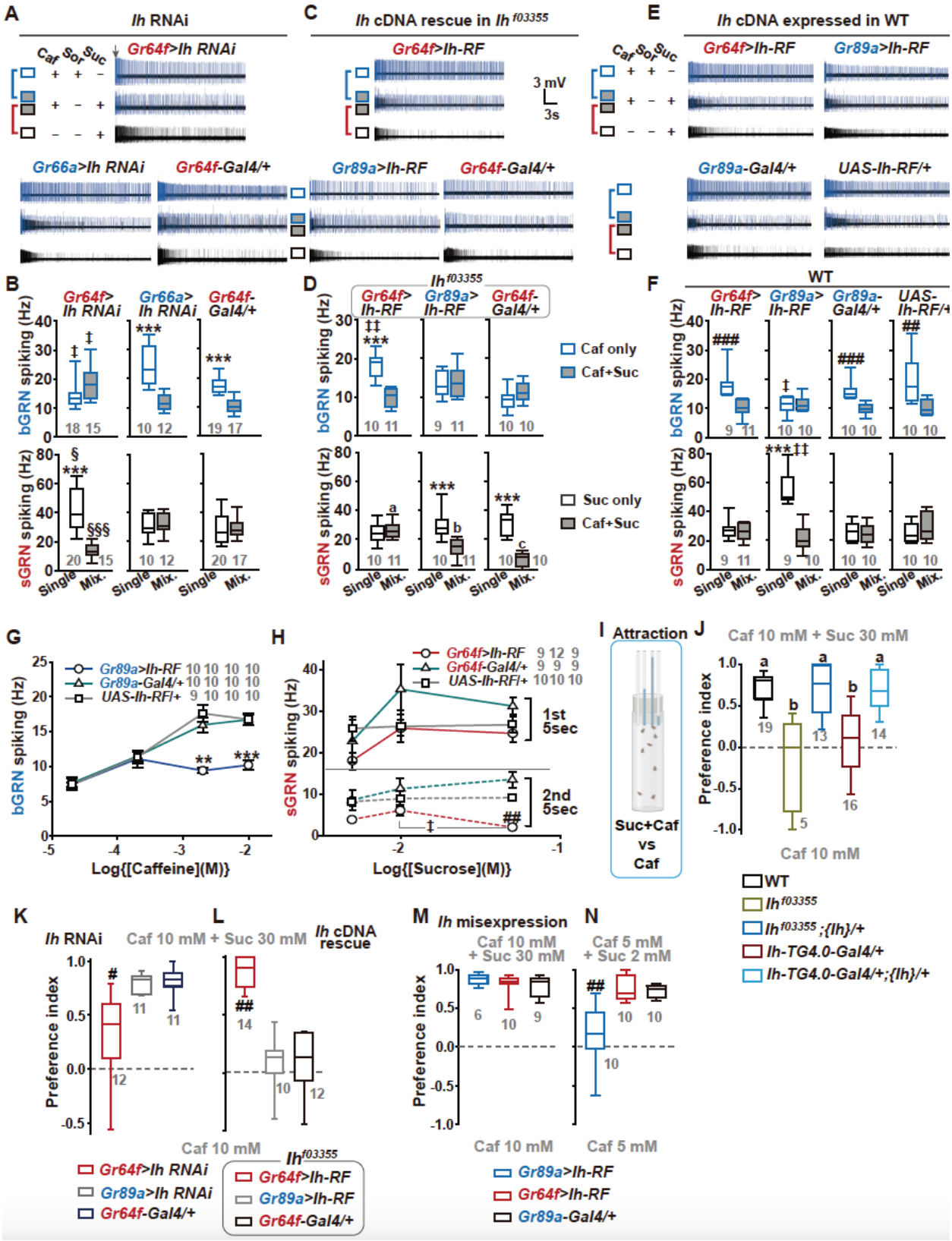
A
Ih RNAi
Caf Sor Suc
Gr64f>Ih RNAi
Gr66a>Ih RNAi
Gr64f-Gal4/+
C
Ih cDNA rescue in Ih f03355
Gr64f>Ih-RF
3 mV
3s
Gr89a>Ih-RF
Gr64f-Gal4/+
E
Ih cDNA expressed in WT
Gr64f>Ih-RF
Gr89a>Ih-RF
Gr89a-Gal4/+
UAS-Ih-RF/+
B
bGRN spiking (Hz)
sGRN spiking (Hz)
Single
Mix.
D
Ih f03355
Caf only
Caf+Suc
Suc only
F
WT
G
Gr89a>Ih-RF 10 10 10 10
Gr89a-Gal4/+ 10 10 10 10
UAS-Ih-RF/+ 9 10 10 10
Log{[Caffeine](M)}
H
Gr64f>Ih-RF 9 12 9
Gr64f-Gal4/+ 9 9 9
UAS-Ih-RF/+ 10 10 10
1st 5sec
2nd 5sec
Log{[Sucrose](M)}
I Attraction
Suc+Caf vs Caf
J
Caf 10 mM + Suc 30 mM
Preference index
Caf 10 mM
WT
Ih f03355
Ih f03355;{Ih}/+
Ih-TG4.0-Gal4/+
Ih-TG4.0-Gal4/+;{Ih}/+
K
Ih RNAi
Caf 10 mM + Suc 30 mM
Gr64f>Ih RNAi
Gr89a>Ih RNAi
Gr64f-Gal4/+
L
Ih cDNA rescue
Ih f03355
Gr64f>Ih-RF
Gr89a>Ih-RF
Gr64f-Gal4/+
M
Ih misexpression
Caf 10 mM + Suc 30 mM
Caf 10 mM
Gr89a>Ih-RF
Gr64f>Ih-RF
Gr89a-Gal4/+
N
Caf 5 mM + Suc 2 mM
Caf 5 mM

Fig. 6. The unilateral interaction mediated by HCN expression in sGRNs allows animals to discern and ingest sweets mixed with bitters. *Gr64f-* and *Gr89a-Gal4* were used to genetically manipulate sGRNs and bGRNs, respectively. (**A** and **B**) Expression of *Ih* RNAi in sGRNs reversed the lateral inhibition like Ih^{f03355} (***: unpaired t-test, $p < 0.001$, between tastant conditions) and reduced bGRN responses to caffeine-only stimulation (‡: Dunn's, $p < 0.05$, §: Welch's ANOVA, Games-Howell test, $p < 0.05$, §§§: Tukey's, $p < 0.001$ between genotypes). (**C** and **D**) Introduction of the *Ih-RF* cDNA in sGRNs (*Gr64f>Ih-RF)*, but not bGRNs (*Gr89a>Ih-RF*), in a Ih^{f03355} background restored sucrose-dependent bGRN inhibition (***, unpaired t-test, $p < 0.001$, between different tastants) and bGRN sensitivity to caffeine-only stimulation (‡‡: Dunn's, $p < 0.01$, between genotypes). (**E** and **F**) Misexpression of *Ih-RF* in bGRNs (*Gr89a>Ih-RF*) of WT reversed the direction of the lateral interaction (##, ###: Mann-Whitney U test, $p < 0.01$, 0.001, respectively. ***: Unpaired t-test, $p < 0.001$), suppressed bGRNs stimulated by caffeine alone, and potentiated sGRN responses to sucrose-only stimulation (‡, ‡‡: Dunn's, $p < 0.05$, 0.01, respectively, between genotypes). Caf, 2 mM; Sor, 50 mM; Suc, 50 mM. (**G**) HCN limits the activity of neurons where it is expressed. HCN misexpression in bGRNs reduced bGRN responses to 2 and 10 mM caffeine (**, ***: Tukey's, $p < 0.01$, 0.001, respectively). (**H**) Overexpression of HCN in sGRNs reduced the sGRN responses to sucrose-only stimulation (##: Dunn's, $p < 0.01$, between genotypes. ‡: Dunn's $p < 0.05$, between 10 and 50 mM sucrose). (**I**) Schematic of the CAFE design for measuring preference index. (**J**) *Ih* deficiency impaired the ability of flies to ingest caffeine-laced sucrose. Letters indicate statistically distinct groups: Dunn's, $p < 0.05$. (**K** and **L**) *Ih* in sGRNs is required for the ingestion of bitter-laced sucrose. (**M** and **N**) Misexpression of *Ih* in bGRNs of WT also impairs ingestion of a sucrose-bitter mixture. #, ##: Dunn's, $p < 0.05$, 0.01, respectively. Gray numbers are n (in the order of the doses in the graphs, G and H).

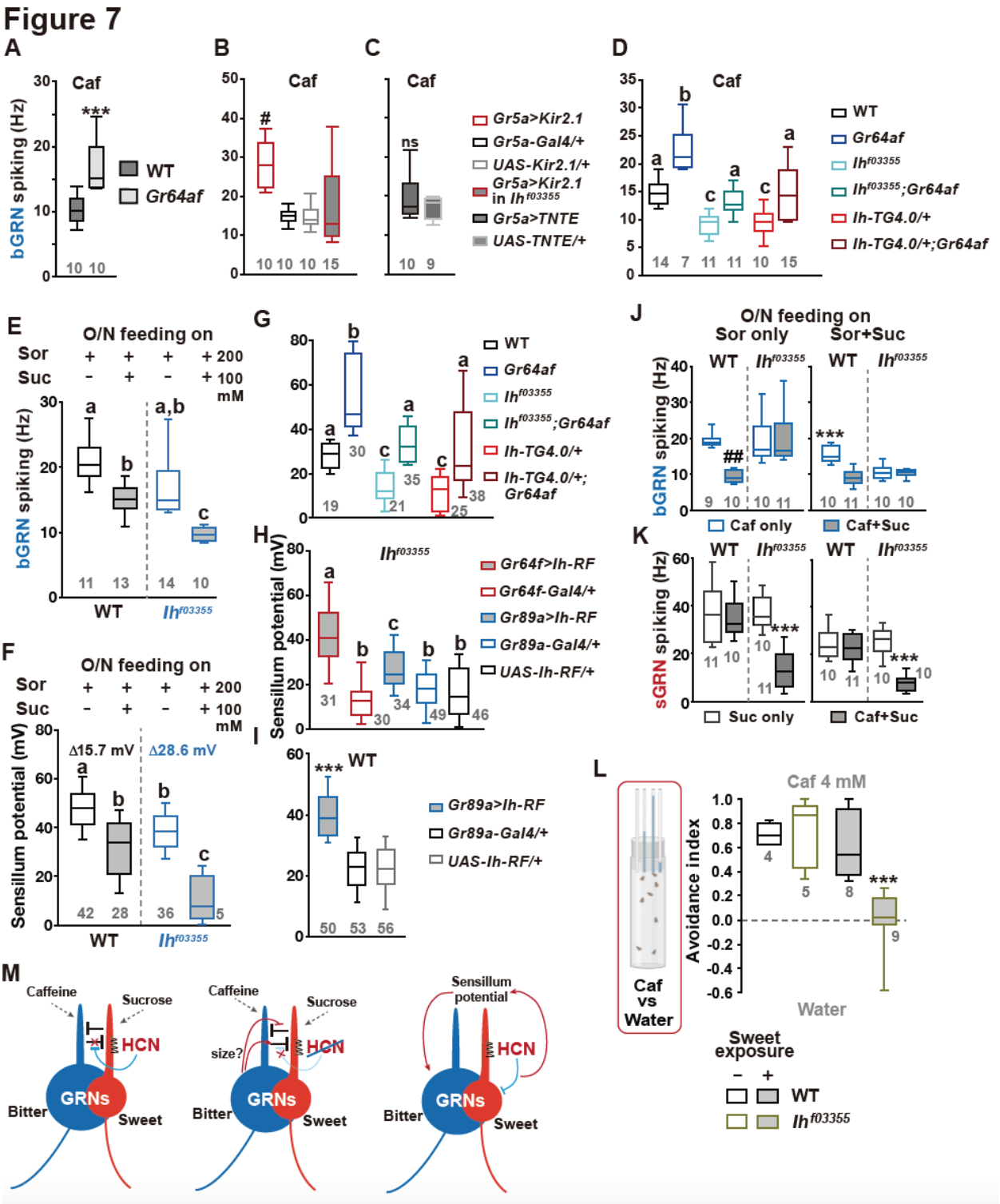

Fig. 7. *Ih* in sGRNs potentiates sGRN-neighboring bGRNs by preserving the sensillum potential. (**A**) Caffeine-evoked bGRN spiking increased in response to the indicated bitters in sucrose-ageusic *Gr64af* mutants. Caf, 0.09 mM. ***: unpaired t-test, $p < 0.001$. See also Figure S7A. (**B** and **C**) Silencing by Kir2.1, but not blocking chemical synaptic transmission, in sGRNs increased the spiking of caffeine-stimulated bGRNs, which was reversed by Ih^{f03355}. Caf, 2 mM. #: Dunn's $p < 0.05$. (**D**) The increased bGRN spiking in *Gr64af* was restored to WT levels by *Ih*

deficiencies. Caf, 2 mM. Letters indicate different groups: Tukey's, $p < 0.05$. (**E**) Sweet media reduced caffeine-induced bGRN spiking. *Ih*^{f03355} was affected by the type of media more severely than WT. Caf, 2 mM. (**F**) The SP of *Ih*^{f03355} bristle sensilla showed the greatest reduction among the indicated treatments, as did bGRN activity in *Ih*^{f03355} after incubation on sweet media (E). See also Figure S7C-H for technical details. (**G**) SP was increased upon sGRN inactivation and reduced by *Ih* loss-of-function. (**H**) The reduced SP of *Ih*^{f03355} sensilla was restored by *Ih-RF* expression in GRNs (red for sGRNs, blue for bGRNs). (**I**) *Ih* misexpression in bGRNs further increased SP, which correlated with increased sucrose-induced sGRN activity (Figure 6F). (**J** and **K**) Sweet fly food affected GRN activity via SP but it did not affect the direction of lateral GRN interactions. Media were prepared as in (E). Caf, 2 mM; Sor, 50 mM; and Suc, 50 mM, were used to trigger GRN spiking. (**L**) *Ih* is required for robust caffeine avoidance for flies maintained on sweet regular food. *Ih*^{f03355} flies avoided 4 mM caffeine like WT flies separated from sweet food for 20 hrs (blank boxes). (**M**) Model for the genetic program of *Ih*-dependent unilateral inhibition that encodes sweetness dominance. Letters indicate statistically distinct groups: a-c, Dunn's, $p < 0.05$ (E,G),Tukey's, $p < 0.01$ (F), or Welch's, Games-Howell test, $p < 0.05$ (H). ***: Tukey's, $p < 0.001$ (I-L). ##: Dunn's, $p < 0.01$. Gray numbers are n.